

Design and modelling of bioinspired 3D printed structures

C. Garrido¹, E. Alabort² and D. Barba¹

¹ Departamento de Materiales y Producción Aeroespacial
E.T.S de ingeniería Aeronáutica y del Espacio
Universidad Politécnica de Madrid
Madrid, Spain
e-mail: conrado.garrido@upm.es
daniel.barba@upm.es

² Alloyed Ltd
Oxford Industrial Park
Yarnton, United Kingdom
e-mail: enrique.alabort@alloyed.com

Key words: Lattice structure, bio-inspired materials, finite element methods models, metamaterials, titanium

Abstract: *Metamaterials are those that, through human engineering, have unusual properties that cannot be commonly found in nature. Recently, these metamaterials have been gaining importance due to the introduction of additive manufacturing technologies. Specifically, metamaterials known as lattice structures have advantages over bulk solid materials, such as increased strength and specific stiffness. However, in order to exploit these advantages of these exotic materials, we need robust and accurate tools to tailor and design their properties. The objective of this work is to present a complete systematic study of the different approaches for metamaterial computational design evaluating their advantages and drawbacks in terms of computational efficiency and accuracy in predicting the metamaterial mechanical properties.*

1 INTRODUCTION

Metamaterials are human designed materials which can acquire unforeseen properties not seen in nature [1]. These can be produced by different manufacturing methods [2]. There are different types of metamaterials, e.g., electromagnetic metamaterials modulating electromagnetic waves [3] or mechanical metamaterials with extraordinary specific mechanical behavior [4]. One type of mechanical metamaterials are lattice structures. Lattices have interesting properties like weight reduction compared to the solid structure, preserving other beneficial properties, for example the strength or biocompatibility [5]. Lattice structures are expected to revolutionize different fields [6],[7]. In the biomedical industry, these structures are selected as the perfect candidate for a new generation of biocompatible implants [6]. In the aerospace industry, the light-weighting potential of these structures can replace solid component with similar properties but higher weights [7]. In order to design these lattice structures, computational simulations are critical. Finite element modelling (FEM) stands as the preferred route to simulate lattice structures. The unresolved problem of using FEA for lattice design resides in the numerous variables that affect the results which can lead to a wrong design-optimization exercise. Among them are the type of mesh, the number of elements or heterogeneities in the material properties heritage from the additive manufacturing process. Furthermore, there is not a systematic study that shows the optimal form of modelling metamaterials [8].

To fill this gap, this work presents a systematic study of the effect of these variables on the mechanical simulations of latticed metamaterials. Three different methodologies are used: 3D explicit meshing, homogeneous beam models and heterogeneous beam models. The computational results are validated against experimental results of a lattice structure explicitly designed

and manufactured for this study.

2 METHODOLOGY OF THE STUDY

2.1 Lattice geometry

For this project, a typical lattice structure has been designed with a strut radius of 1.3 mm and target solid fraction of 24% following a Voronoi distribution, see Fig. 1. A summary of lattice structure features is presented in Table 1. The design has been additively manufactured (AM) by selective laser method in Renishaw AM250 using Ti6Al4V as base material. These are presented in Fig. 2.



Figure 1: Lattice structure used in this study.

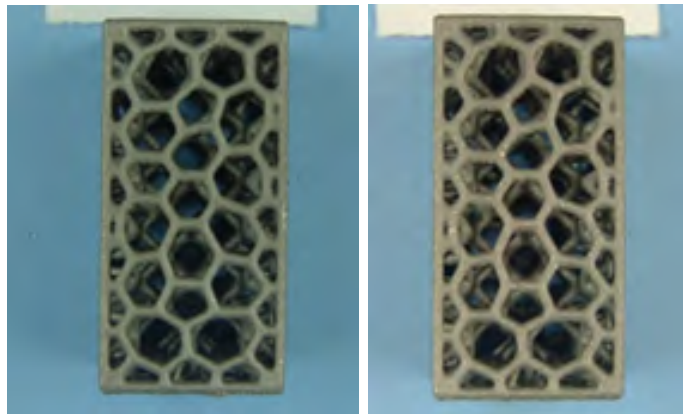


Figure 2: Additively manufactured Ti6Al4V lattice structures.

Structure	Strut radius	Solid fraction
Lattice	1.3 mm	23.78%

Table 1: Features of the lattice structure.

2.2 Mechanical Testing

The additively manufactured lattice samples have been subjected to compression testing using a servo-hydraulic MTS (model 810) universal testing machine equipped with a 100kN load cell. A strain rate of 10^{-3} s^{-1} was imposed during the test. Strain was monitored using digital image correlation (DIC) during the test. The DIC system have a camera (model BFS-U3-13Y3C-C) and also have a in-house code developed to group stress and strain points in real time. Two repeats were performed to address the consistency of the experimental results.

2.3 Computational study

The mechanical behaviour of the lattice structure has been addressed computationally. Abaqus (2018) FEM static analysis has been used for this purpose [9]. The lattice structure has been meshed with 2 different element types: (1) C3D10 volumetric quadratic elements and (2) quadratic B32 beam elements. Table 2 shows the number of elements for each type of mesh. Regarding the boundary conditions, the displacement of the nodes located at the lower face of the sample are restricted in all directions ($U1 = U2 = U3 = 0$). For the nodes at the upper face, a displacement equivalent to 5% of the total sample deformation is imposed. In terms of material model, material properties for the FE model are extracted from the experimental mechanical behaviour of AMTi6Al4V. A wire of AMTi6Al4V with the same thickness of the lattice struts (1.3 mm) was tested in a tension test and the experimental stress-strain curve was used as an Abaqus material database for the lattice structures [10].

Type of Mesh	Number of elements
Volumetric Mesh (C3D10 Abaqus Code)	462551
Beam Mesh (B32 Abaqus Code)	1051

Table 2: Number of elements for volumetric and beam meshes.

A typical feature of these lattice structures is the rounding of the struts at the lattice nodes to avoid stress concentrations promoting premature failures of the lattice, see Fig. 3. Due to this, the radius is not homogeneous along the axis of the struts. The strut radius is higher when approaching to nodes than in the centre of the lattice beams.

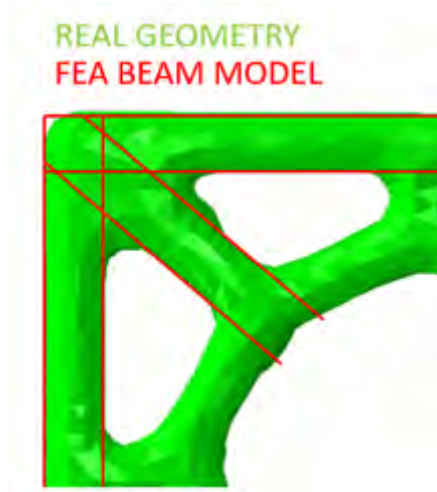


Figure 3: Representation of the curvature produced near the nodes.

The geometry at the nodes of the volumetric models is fully heritage from the explicit lattice structure model in the form of “*stl*” surface. However, for the beam models, the beam radius needs to be estimated in order to obtain a homogenised representative geometry of each strut in the lattice. In this work, two different approaches to target this problem have been proposed (see Fig. 4): (1) model A, assuming the lattice as a continuous beam network with a total volume equal to the experimental one or (2) model B, integrating the effect of the nodes idealising the lattice structure as a combination of beams (struts) and spheres (nodes). The details for each model are explained next. Beam model A: The first model assumes a network of beams with an idealised circular section of area πR_A^2 , see Fig. 4. The total volume V_A of the beam network is calculated as:

$$V_A = \sum_i^N \pi R_A^2 L_A^i \quad (1)$$

Where L_A^i is the node-to-node length of the beam i and N is the total number of beams. By equaling this V_A to the real volume of the AM geometry V_{AM} , the R_A can be extracted as

$$R_A = \sqrt{\frac{V_{AM}}{\pi L_T}} \quad (2)$$

Where L_T is the total length of all beams of the structure. This radius R_A is used to define the section of the beams in model A. The calculated value is presented in Table 3. Beam model B idealises each node as a sphere of radius R_B and each beam as a cylinder of the same radius R_B , see Fig. 4. The total volume of the lattice V_B can be calculated adding up the individual volume of all the nodes and beams in the lattice as:

$$V_B = \frac{4}{3} N_n \pi R_B^3 + \sum_i^N (L_B^i - 2R_B) \pi R_B^2 \quad (3)$$

where LB is the node-to-node length of the strut i and N_n is the total number of nodes in the lattice structure. By equating this V_B to the real volume of the AM geometry V_{AM} , the R_B can be extracted solving the function:

$$R_B = \frac{4}{3}N_n\pi R_B^3 + L_T\pi R_B^2 - 2R_B^3N_B \quad (4)$$

Where N_B is the total number of beams in the structure. This radius R_B is used to define the section of the beams in model B. The calculated value is presented in Table 3.

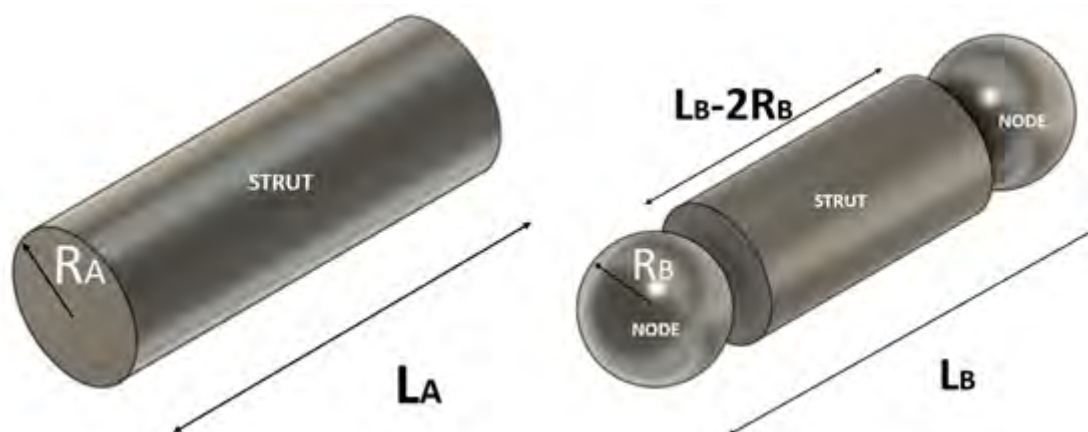


Figure 4: Beam model A (left) and beam model B (right).

Type of Models	Radius (mm)
Experimental at the centre of the struts	0.65
Model A (RA)	0.63
Model B (RB)	0.712

Table 3: Radius for each of the beam models used.

3 RESULTS AND DISCUSSION

In this section, the computational mechanical behaviour of the lattice structure is compared against the experiments. Next, the accuracy of each of the different modelling approaches is addressed. Finally, the advantage and disadvantages of each method are discussed.

3.1 Experimental behaviour

Experimental and FEM stress-strain curves of the lattice structure are presented in Fig. 5. The two repeats of the experimental tests present a good repeatability with less than 10% discrepancy between both curves. The lattice behaviour presents an initial elastic region with an elastic modulus proportional to the solid fraction of the lattice. After yielding, there is an initial hardening region followed by a plateau before failure (not studied in this work). The three different FEM approaches (Volumetric, Beam Model A and Beam Model B) present a similar qualitative behaviour. However, quantitatively, the three models differ, with the volumetric model presenting the closest behaviour to the one experimentally observed.

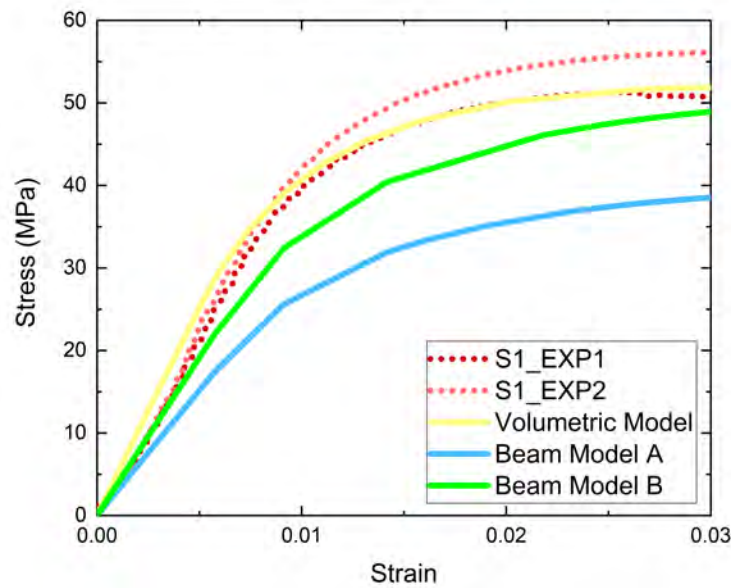


Figure 5: Experimental and FEM stress-strain curves. Red curves represent experimental lattice compression test, yellow curve represents the volumetric model and blue and green curves represent the beams models A and B, respectively.

The apparent elastic modulus and yield stress has been extracted from the stress-strain curves; they are shown in Fig. 6. The apparent elastic modulus of the volumetric model is higher than the experimental ones ($\sim 10\%$ higher) while the beam models present a substantially lower elastic modulus than the experiments ($\sim 30\%$ lower for Model A and $\sim 20\%$ lower for Model B). Regarding the higher rigidity of the volumetry model when compared to the experiments, it is known that AM lattice present defects, especially for self-supported lattices like the ones in this work [11]. These defects can reduce rigidity of the lattice and might partially explain the small increase in the elastic modulus, which are not taking into account in the models. Another reason might be small deviations in the printed geometries from the ideal simulated ones [11]. In terms of the yield stress, all the models present lower values than the experimental ones. The volumetric and beam model B present the closest values to the experiments ($< 10\%$ error) while the beam model A differs considerable ($> 20\%$ lower yield strength). As a summary, the volumetric model shows superior accuracy when comparing with the experimental apparent elastic modulus and yield stress. On the other hand, beam model A presents the worst approximation for both, the apparent elastic modulus and the yield stress.

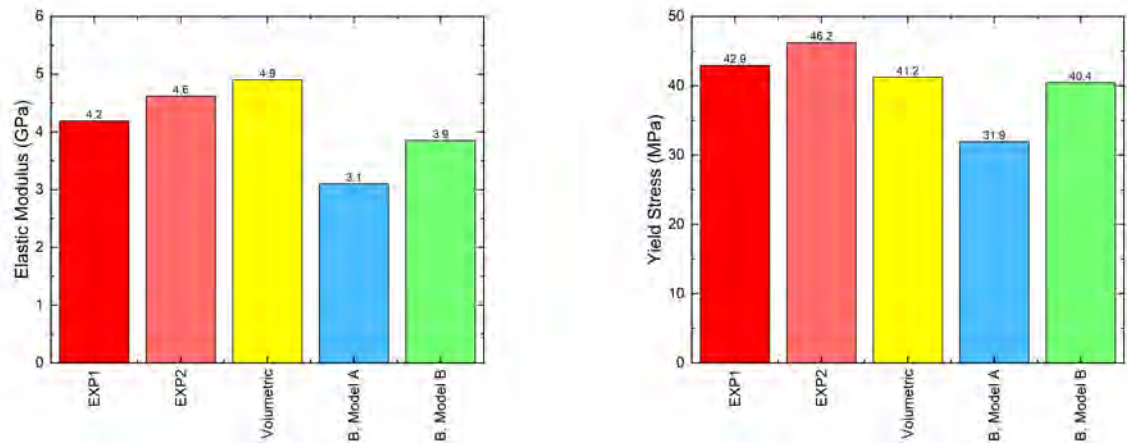


Figure 6: Experimental and FEM elastic modulus (left) and yield stress (right).

The mechanical behaviour of lattice structures is strongly influence by their solid fraction [12]. Small deviations of the solid fraction can produce significant variations in the mechanical behaviour of the lattice. Therefore, it is important to address this aspect between the experiments and the simulations. Solid fractions of experimental and FEM geometries are compared in Fig. 7. There are small deviations between the computational geometry (ideal design geometry) and the experimental one, arising from the imperfections in the additive manufacturing process [13]. Beam model A has the same solid fraction than the volumetric model because the radius is obtained equalling AM structure volume and beam model volume. On the other hand, beam model B has the bigger solid fraction due to the overlap of the beams produced at the nodes.

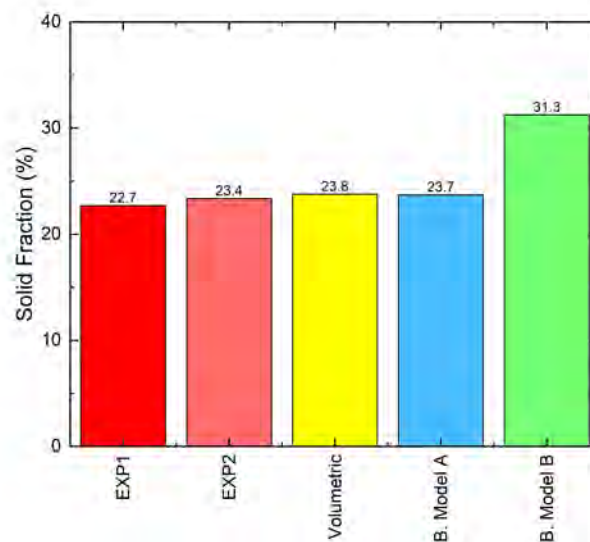


Figure 7: Solid fraction estimated for the samples tested and the numerical models, respectively.

3.2 Failure modes

In this section, focus is put on the failure mechanisms in the lattice structure. Fig. 8 shows the failure modes of each model compared to the experimental specimen. Volumetric failure modes correlate well with the ones observed experimentally. Both beam models (A and B) present the same failure modes, suggesting that the change in beam diameter between A and B did not affect the failure mechanism.

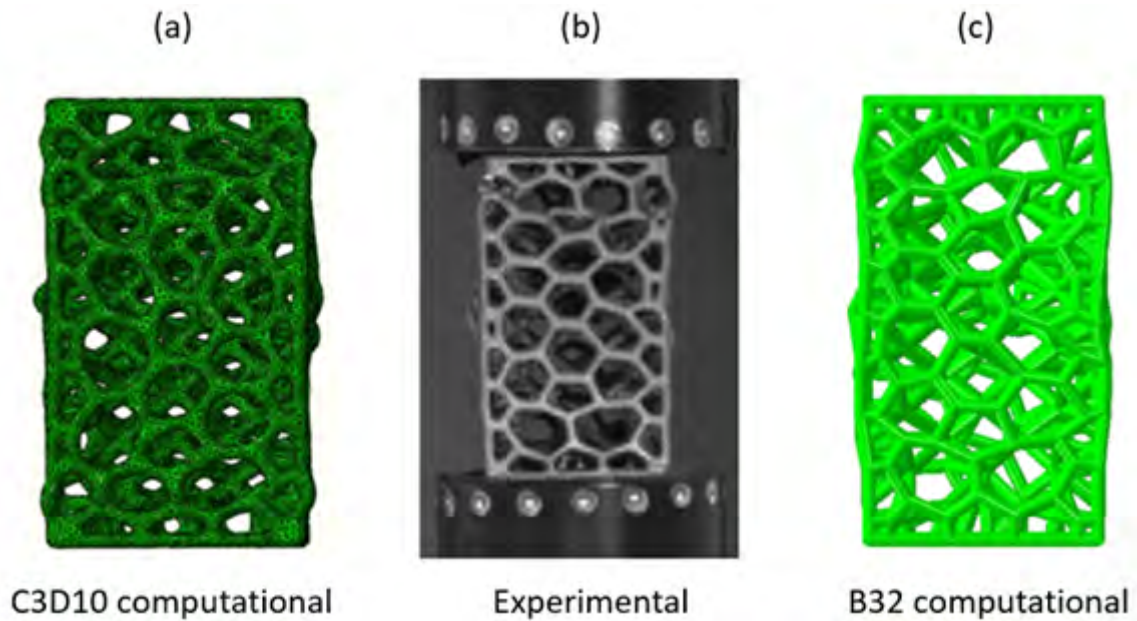


Figure 8: Comparison between failure modes in the volumetric model (a), experimental specimen (b) and the beam models (c).

3.3 Computational efficiency and discussion

Computational cost is a critical aspect in the design of lattice structures. In this regard, the computational time of each FEM approach is represented in Fig. 9. Beam models have considerably lower computational cost than the volumetric model. This supports the necessity of developing new beam theories adapted to AM lattice design capturing the peculiarities and defects in these structures.

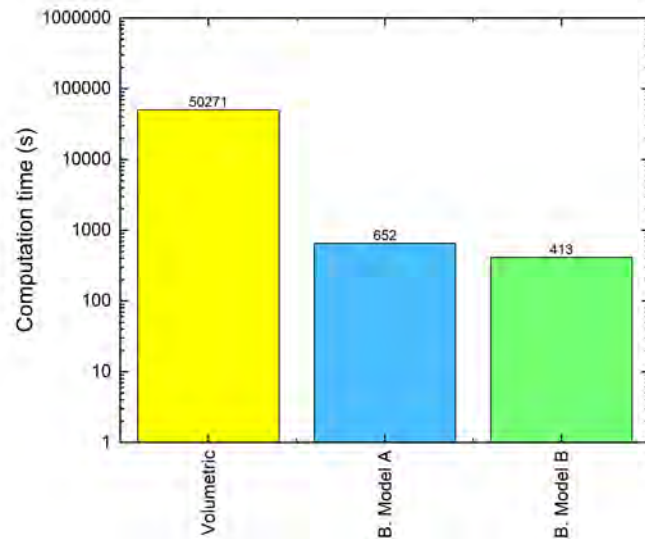


Figure 9: Computation time of FEM models.

4 CONCLUSIONS

In this work, the advantages and drawbacks of different FEM approaches in modelling and design AM metamaterial structures have been studied. The following conclusions can be drawn:

- Volumetric FE models with elasto-plastic material equations present the best accuracy when compared to experimental results. The minor difference in the mechanical response between experimental specimens and FE volumetric models are due to the defects present in the experimental specimens that have not been considered in the simulations. These models capture the plastic failure mechanics with great accuracy. However, these models present higher computational costs than beam models.
- Two criteria to establish FE radius in beam models have been presented: one based on the total experimental volume of the lattice (model A) and another simulating the lattice structure as combination of struts and spheres (model B). The beam model B presents a higher accuracy than model A. The beam model B has an error less than 10% compared to experiments in elastic modulus and yield stress.
- Beam models are computationally more efficient than volumetric models. However, the precision of these models is lower, and they do not correctly maintain the physics of the deformations. There is a need to develop new beam models that capture the same physics than volumetric models but with a lower computational cost.

REFERENCES

- [1] T. J. Cui, D. R. Smith, and R. Liu, *Metamaterials*. Springer, 2010.
- [2] Y. Ding, M. Akbari, X.-L. Gao, L. Ai, and R. Kovacevic, “Use of powder-feed metal additive manufacturing system for fabricating metallic metamaterials,” in *Manufacturing techniques for materials: engineering and engineered*, pp. 51–65, CRC Press, 2018.
- [3] R. M. Walser, “Electromagnetic metamaterials,” in *Complex Mediums II: beyond linear isotropic dielectrics*, vol. 4467, pp. 1–15, International Society for Optics and Photonics, 2001.
- [4] X. Zheng, H. Lee, T. H. Weisgraber, M. Shusteff, J. DeOtte, E. B. Duoss, J. D. Kuntz, M. M. Biener, Q. Ge, J. A. Jackson, *et al.*, “Ultralight, ultrastiff mechanical metamaterials,” *Science*, vol. 344, no. 6190, pp. 1373–1377, 2014.
- [5] X. Yan, Q. Li, S. Yin, Z. Chen, R. Jenkins, C. Chen, J. Wang, W. Ma, R. Bolot, R. Lupoi, *et al.*, “Mechanical and in vitro study of an isotropic Ti6Al4V lattice structure fabricated using selective laser melting,” *Journal of Alloys and Compounds*, vol. 782, pp. 209–223, 2019.
- [6] D. Mahmoud and M. A. Elbestawi, “Lattice structures and functionally graded materials applications in additive manufacturing of orthopedic implants: a review,” *Journal of Manufacturing and Materials Processing*, vol. 1, no. 2, p. 13, 2017.
- [7] G. Totaro and Z. Gürdal, “Optimal design of composite lattice shell structures for aerospace applications,” *Aerospace Science and Technology*, vol. 13, no. 4-5, pp. 157–164, 2009.
- [8] Z. Li, C. Wang, and X. Wang, “Modelling of elastic metamaterials with negative mass and modulus based on translational resonance,” *International Journal of Solids and Structures*, vol. 162, pp. 271–284, 2019.
- [9] E. Giner, N. Sukumar, J. Tarancón, and F. Fuenmayor, “An abaqus implementation of the extended finite element method,” *Engineering fracture mechanics*, vol. 76, no. 3, pp. 347–368, 2009.
- [10] G. F. de Vera Conrado and B. C. Daniel, “Smart modelling of additively manufactured metamaterials,” in *2020 IEEE 10th International Conference Nanomaterials: Applications & Properties (NAP)*, pp. 02SAMA18–1, IEEE, 2020.
- [11] D. Barba, C. Alabort, R. C. Reed, and E. Alabort, “On the size effects in additively manufactured titanium and the implications in am components,” in *TMS 2020 149th Annual Meeting & Exhibition Supplemental Proceedings*, pp. 449–456, Springer, 2020.
- [12] C. Chu, G. Graf, and D. W. Rosen, “Design for additive manufacturing of cellular structures,” *Computer-Aided Design and Applications*, vol. 5, no. 5, pp. 686–696, 2008.
- [13] B. Wu, Z. Pan, D. Ding, D. Cuiuri, H. Li, J. Xu, and J. Norrish, “A review of the wire arc additive manufacturing of metals: properties, defects and quality improvement,” *Journal of Manufacturing Processes*, vol. 35, pp. 127–139, 2018.